35th Annual International Conference of the IEEE EMBS
Osaka, Japan, 3 - 7 July, 2013

Current Steering for High Resolution Retinal Implants

N.L. Opie[1,2], N.H. Lovell[2], G.J. Suaning[2], P. Preston[2], S. Dokos[2]

Abstract—**To significantly increase the resolution achievable by a retinal prosthesis without requiring additional electrodes, a current steering technique could be utilized. In this study, a finite element model was constructed to analyze the local concentrations of charge carrying ions within a saline bath due to concurrent stimulation from two electrodes surrounded by a hexagonal arrangement of return electrodes. By altering the return pathways, tissue activation and identification of unique stimulation patterns is possible. Ag/Ag-Cl electrodes and a voltage controlled current source were developed to validate the finite element model, with the model accurately predicting saline bath measurements. The average error in the returned currents between the finite element model and experimental results was 2% relative to the stimulus current.**

I. Introduction

One of the main technical and scientific barriers in the development of a retinal prosthesis is to provide the patient with high resolution vision. Current clinical trials as well as simulations performed using normally sighted subjects suggest that in excess of 1000 electrodes may be required to provide mobility, facial recognition and the ability to read [1-4]. However, no implantable devices with large numbers of electrodes are commercially available. In fact, there are few neurostimulation devices that have effectively coupled hundreds or thousands of stimulation channels to excitable tissue and maintained this interface over the long-term. To reduce the number of electrodes required without reducing the potential of achieving high resolution vision, it is possible that multiple electrodes could be used simultaneously to steer the injected currents and create virtual electrodes at desired tissue locations. Such current steering techniques have been successful in inducing virtual electrodes in cochlear implants and for deep brain stimulation [5,6].

This work investigates the ability of using combinations of return electrodes to steer current, creating regions of potential tissue activity that can be identified and differentiated using only a small number of electrodes. Further, we are investigating the ability of a three-dimensional finite element model (FEM) to predict the paths of current returning from a central stimulating electrode to combinations of distant return electrodes, qualitatively validating these findings with similar recordings made using silver/silver-chloride electrodes immersed in a saline bath. In this model, two stimulating electrodes are surrounded by six return electrodes in a hexagonal lattice [7]. By choosing combinations of return electrodes, current densities between the electrodes are expected to vary, resulting in different patterns of neural activation. While these different patterns may not implicitly represent a particular number or letter, the ability of persons to learn to read using symbols (dots and dashes) has been demonstrated successfully with Morse code and Braille, and it is thus plausible that patients implanted with a retinal prosthesis may be able to learn to read using an alternative alphabetic code.

Our model theoretically predicts the amount of current returned through a predetermined set of return electrodes and simulates the extracellular potential experimentally observed within a saline bath. Thus, the ability of using particular sets of return electrodes to steer current through the saline bath to produce specific regions of activation is analyzed by the current returning to each of the electrodes within the chosen set. These return currents, validated by experimental measurements, indicate that it is plausible to inject currents of magnitudes that do not cause tissue or electrode damage, yet will be sufficient to elicit neural responses.

II. Methodology

A. Finite Element Model

A three-dimensional FEM was developed using COMSOL Multiphysics 4.1.0.88 (COMSOL AB, Sweden) to emulate current flowing through a saline bath. In this design, two hexagonal clusters comprising a total of fourteen electrodes were utilized. Electrodes within the array were designated as either stimulating or return electrodes. Stimulating electrodes were positioned centrally within the hexagonal clusters and connected to one of two separate current sources, and the return electrodes were connected to a zero potential. The model was formulated using hemispherical electrodes of 0.4 mm radius, immersed in a 2 mm deep saline tank measuring 6.50×4.25 mm^2. The mathematical model assumed that the voltage distribution (v) throughout the saline bath was governed by the Laplace relation (1)

$$-\nabla \cdot (\sigma \nabla V) = 0 \qquad (1)$$

where σ (S/m) is the conductivity of the physiological saline medium [8]. By assuming the electrodes were hemispherical, and the physiological saline had a constant conductivity of 1 S/m [9], equation (1) could be reduced to the partial differential system

*This research was supported in part by the Australian Research Council (ARC) through its Special Research Initiative (SRI) in Bionic Vision Science and technology grant to Bionic Vision Australia (BVA).

[1]Centre for Eye Research Australia, Royal Victorian Eye and Ear Hospital, The University of Melbourne.

[2]Graduate School of Biomedical Engineering, University of New South Wales.

Email: nicholas.opie@unimelb.edu.au.

$$\frac{\partial^2 V(x,y,z)}{\partial x^2} + \frac{\partial^2 V(x,y,z)}{\partial y^2} + \frac{\partial^2 V(x,y,z)}{\partial z^2} = 0 \quad (2)$$

with boundary conditions

$$V = 0 \quad (3)$$

at all return electrodes and

$$\frac{\partial V}{\partial n} = \frac{I}{2\pi r^2} \quad (4)$$

where i (mA) is the magnitude of current injected into the stimulating electrodes, and r (mm) is the electrode radius. Zero flux boundary conditions

$$\frac{\partial V}{\partial n} = 0 \quad (5)$$

were imposed on the edges of the saline bath. In (4) and (5), $\partial/\partial n$ denotes the derivative along the direction of the outer normal to the saline bath boundary. Over 50,000 tetrahedral elements were used in the meshing of the saline bath and spherical electrodes. Electrodes 4 and 11 (E4 and E11), shown in Fig. 1, were the designated stimulating electrodes and were both injected with currents of 1 mA.

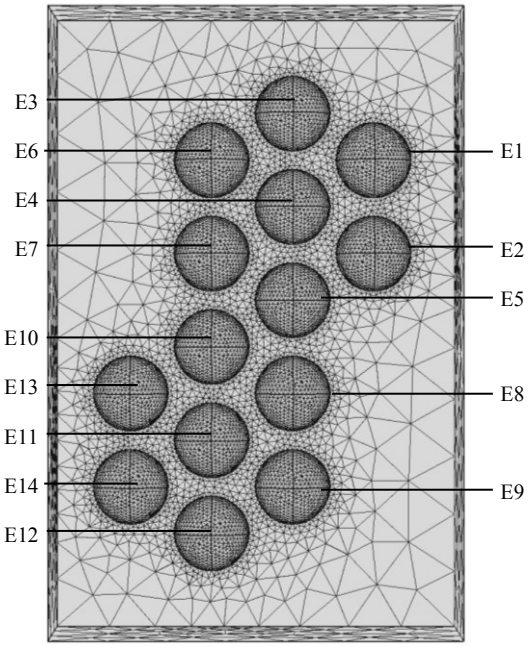

Fig 1. Schematic diagram of the constructed 6.50 x 4.25 mm^2 saline bath, indicating the location of each of the spherical Ag-AgCl electrodes and the mesh elements used in the FEM analysis. Electrodes E4 and E11 were designated to be stimulating electrodes, being placed centrally to a hexagonal cluster of return electrodes.

B. Electrode Array and Current Source

A fourteen electrode (two ring) hexagonal electrode array was fabricated by heating a 0.3 mm diameter, 99.9% Ag wire by means of a butane torch. As the silver heated up, the surface tension of the molten metal pulled the wire into a ball, with diameters that could be reasonably well controlled by the time and length of wire that was heated. Electrodes were then immersed in commercial bleach (3.5% w/v sodium hypochlorite) for 15 minutes, coating the electrodes in an AgCl shell. To test the finite element computational model, a 2 mm deep, 6.50 × 4.25 mm^2 saline bath was constructed. Fourteen, 0.35 mm electrode holes were drilled through a printed circuit board (PCB) board in a 1 mm center-center separated hexagonal pattern. The saline bath was coated in a 50 µm thick coating of silicone sealant (Permatex, CT; Type 65AR flowable) to prevent water leakage and absorption by the PCB, which was filled to a depth of 2 mm with physiological saline (0.9% NaCl, Promed, Australia). Spherical electrodes with an average diameter of 391 ± 20 µm were threaded through the holes while the silicone cured, and were soldered to connection pads on the opposite side.

To pass currents through the electrodes within the saline bath, a voltage controlled current source (VCCS) was developed and connected to a signal generator with a 1 kHz sinusoidal waveform and a regulated ±15 V power supply. The voltage controlled current source used TL072 operational amplifiers and a 5 kΩ variable resistor to deliver currents between 0.1 and 1.1 mA from the two stimulating electrodes (E4 and E11) through the physiological saline to the return electrodes (E1, E2, E3, E5, E6, E7, E8, E9, E10, E12, E13 and E14), with currents obtained by measuring the voltage drop measured across 0.1%, 1 kΩ sense resistors. To remove all DC current flowing through the electrodes, a DC bypass system was also employed.

C. Saline Bath Testing

To test whether the finite element model could accurately predict current flow in response to various return configurations, ten sets of return electrode combinations (A-J) were chosen and used, with configurations indicated in Fig. 2. For each test, a current of 1 mA was supplied to each of the central stimulating electrodes as a continuous 1 kHz sinusoidal signal. Measurement of the current magnitude returned through each of the utilized return electrodes was compared to the finite element model simulations.

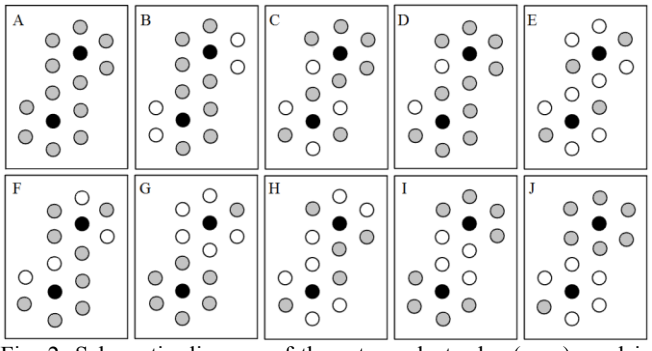

Fig. 2. Schematic diagram of the return electrodes (grey) used in each of the ten trials. Black circles represent the central stimulating electrodes and open, white circles indicate inactive electrodes that were not utilized.

III. Results And Analyses

A. Finite Element Model Simulations

Results of voltage distribution from FEM simulations conducted with ten different return electrode combinations are shown in Fig. 3., for equal, 1 mA currents injected into each of the central stimulating electrodes. These images indicate that the majority of charge injected from the central stimulating electrodes will be restrained within the hexagonal electrode clusters, forming different patterns of expected activation based on the different combinations of return electrodes used. Further, combinations of inactive electrodes can be used to induce cross-talk, with charge flowing from one stimulating electrode to return electrodes of the opposite hexagonal cluster (Fig. 4G, and Fig.4 J). It is expected that it would be possible to represent numbers and letters using electrical stimulation through the use of these activation patterns and current spread.

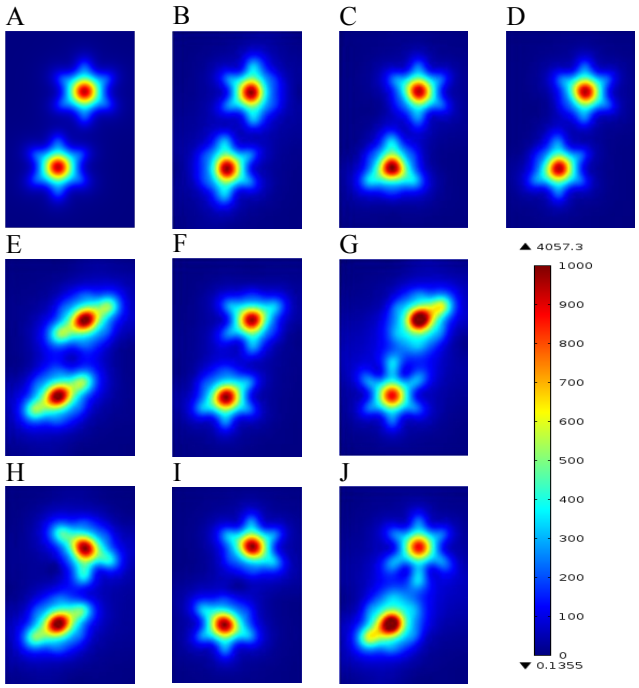

Fig. 3. FEM predictions of voltage distribution from each of the ten return electrode combinations used taken at a depth of 400 μm, the apex of the electrodes. Scale is in mV.

The currents observed by the model to be returned through each of the return electrodes are listed in Table I, for a total injection current of 2 mA (1 mA per central stimulating electrode). In each simulation, currents are generally largest in the electrodes that are situated between the two central stimulating electrodes (E5, E7, E8 and E10). Results obtained from uneven combinations of return electrodes, such as combinations G and J, indicated that a large proportion (43.4% in combinations G and J) of the current supplied to the hexagonal cluster with fewer electrodes would be steered to return electrodes within the opposite cluster. A further assessment of the electrode similarity can be made using combination A (all electrodes) in which opposite pairs can be matched and compared (electrodes E1-E14, E2-E13, E3-E12, E5-E10, E6-E9 and E7-E8), with the theoretical model predicting equivalent current returns through each electrode within the pair.

B. Experimental Results

The currents measured through each of the return electrodes from two simultaneous 1.0 mA current injections (through the two central, stimulating electrodes), and the percentage of the experimentally measured return current (as a fraction of the FEM simulated currents) are listed in Table I for each of the return electrode combinations examined.

In each experiment, similar to results observed during the FEM simulations, larger currents were observed in the electrodes situated between the two central stimulating electrodes (E5, E7, E8 and E10).

C. Comparison between Experimental Results and FEM

When comparing the current returned to the electrodes between the FEM simulations and the experimental measurements, there was a difference of less than 1% of the total injected current (20 μA) in 36.4% of the electrodes from all trials (28 of 77 electrodes), less than 2% (40 μA) in 33.8% (26/77), less than 5% (100 μA) in 22.0% of trials (17/77) and a difference of more than 100 μA between the theoretical FEM predictions and the experimental results in only 7 cases (7.8% of all electrodes). The average difference between the saline bath experiments and the finite element model simulations for all electrodes and combinations was 39.5 μA, less than 2% of the total charge injected. In most cases, the currents are returned equivalently to each hexagonal cluster, however, with electrode combinations G, H and J, which did not have active return electrodes between the two stimulating electrodes, current spread between the two clusters was not as effectively predicted.

In both sets G and J, a full hexagonal cluster (all electrodes) was employed in conjunction with one electrode from the opposite hexagonal cluster. As these electrode sets were equal and opposite, the currents returns should also have been equivalent. It was observed, however, that the single electrodes had significantly different current returned (E14 returned 274 μA in combination G, and E1 returned 340 μA in combination I), which may be indicative that the experimental electrodes were not in perfectly symmetrical locations, with electrode E14 potentially closer to hexagonal cluster 1 than E1 was to hexagonal cluster 2.

Results also indicated that by configuring the utilized return electrodes, a large proportion of charge could be spread to the neighboring hexagonal cluster. For combinations G and J, 86.3% (1724 μA) and 17.0% (340 μA) of the total injected current was returned to hexagonal cluster 1, indicating a transfer of 724 μA and 658 μA between the clusters, respectively.

IV. Discussion

Overall, the electrode array and voltage controlled current source was shown to be effective in investigating the spread of current through a saline bath. A method of manufacturing cheap and simple electrodes, sufficient to investigate current

TABLE I. CURRENTS RETURNED FOR EACH ELECTRODE THROUGH FEM SIMULATIONS AND SALINE BATH EXPERIMENTS

	Return Electrode Configuration	Current returned through FEM simulations / saline bath experiments (μA) (Percentage Ratio (%))									
		A	B	C	D	E	F	G	H	I	J
	E1	167/152		324/312	225/176	485/510	263/238	195/250	464/390	217/236	567/340
		(110)	-	(104)	(128)	(95)	(111)	(78)	(119)	(92)	(167)
	E2	167/164						239/274		284/260	
		(102)	-	-	-	-	-	(87)	-	(109)	-
	E3	168/148	283/230		186/188		211/238	194/268		219/240	
		(114)	(123)	-	(99)	-	(89)	(72)	-	(91)	-
Hex 1	E5	163/190	262/294	309/202	233/244			318/338			
		(86)	(89)	(153)	(95)	-	-	(94)	-	-	-
	E6	169/158	227/234	320/192	185/198		214/224	213/274		279/312	
		(107)	(97)	(167)	(93)	-	(96)	(78)	-	(89)	-
	E7	165/182	224/262		182/212	514/576	249/274	271/274	422/432		
		(91)	(85)	-	(86)	(89)	(91)	(85)	(98)	-	-
	Total	999/994	996/1020	953/706	1011/1018	999/1086	937/974	1430/1724	886/822	999/1048	567/340
	E8	165/180	225/236			514/506	240/256				271/346
		(92)	(95)	-	-	(102)	(94)	-	-	-	(78)
	E9	169/158	228/230	235/232	226/202		263/236		424/372	279/250	214/260
		(107)	(99)	(101)	(112)	-	(111)	-	(114)	(112)	(82)
	E10	163/190	262/290	236/410	207/236		257/304		339/450		318/278
		(86)	(90)	(58)	(88)	-	(85)	-	(75)	-	(114)
Hex 2	E12	168/146	284/228	190/208	186/184					219/228	194/232
		(115)	(125)	(91)	(101)	-	-	-	-	(96)	(84)
	E13	167/162		195/234	183/190				346/356	283/256	237/292
		(103)	-	(83)	(96)	-	-	-	(97)	(111)	(81)
	E14	167/166		186/212	182/174	482/408	300/228	565/274		216/218	194/250
		(101)	-	(88)	(105)	(118)	(132)	(206)	-	(99)	(78)
	Total	999/1002	999/984	1042/1296	984/986	996/914	1060/1024	565/274	1109/1178	997/952	1428/1658
Hex 1 total current (%)		50.0/49.8	49.9/50.9	47.8/35.3	50.7/50.8	50.1/54.3	46.9/48.7	71.7/86.3	44.4/41.1	50.1/52.4	28.4/17.0

magnitudes observed saline bath experiments was verified. Experimental results from this work indicated the ability to use different combinations of return electrodes to manipulate the spread and return pathways of the injected current through the saline bath. By steering sufficient magnitudes of current in this manner, it is expected that specific patterns of neuronal activation may be possible, which could result in perceptions of numbers and letters.

FEM simulations were utilized and shown to be an accurate representation of currents flowing through the saline bath, and potentially, through neural tissue. Further, the model can be used to graphically represent voltage distributions between electrodes, and indicated that electric potentials due to different return electrode combinations was possible and could be used to steer currents to desired neural regions. While it is expected that differences in the model and the experimental results could be explained by differences in electrode spacing, caused by experimental variation in electrode diameters and the precise locations of the feed-throughs, this was not assessed. Differences in returned currents could also be induced by mismatches in electrode-saline interface impedances, which were neglected in the simulations.

V. CONCLUSION

Despite intense research in retinal prostheses, there is a paucity of data on concurrent stimulation of excitable tissue. While the models and bath testing presented here are rudimentary, our results highlight the significance of interactions between multiple current sources and the importance of electrode design in harnessing potential cross talk. It is evident from the simulations and the good overall agreement with the experimental results, that by choosing appropriate electrode combinations, activation of particular retinal regions should be possible and may enable greater visual resolution without increasing the required number of electrodes.

REFERENCES

[1] D. Yanai, J. D. Weiland, M. Mahadevappa, R. J. Greenberg, I. Fine, M. S. Humayun. "Visual performance using a retinal prosthesis in three subjects with retinitis pigmentosa," *Amer. J. Ophthalmol.,* vol. 143, no. 5, pp 820-827, 2007.

[2] E. Zrenner, "Subretinal implants allow blind RP patients to read letters and combine them to words at once without training" *The Eye and the Chip World Congress on Artificial Human Vision*, Detroit, MI, 2010

[3] R. W. Thompson, G. D. Barnett, M. S. Humayun, G. Dagnelie, "Facial recognition using simulated prosthetic pixelized vision," *Invest. Ophthalmol. Vis. Sci.*, vol. 44, no. 11, pp 5035-5042, 2003.

[4] K. Cha, K. W. Horch, R. A. Normann, "Mobility performance with a pixelized vision system:, *Vision Research*, vol. 32, no. 7, pp. 1367-1372, 1992

[5] C. T. M. Choi, Y. Lee, Y. Tsou, "Modeling deep brain stimulation based on current steering scheme", *IEEE Trans. on Magnetics*, vol. 47, no. 5, pp. 890-893, 2011

[6] X. Lou, "Pitch contour identification with combined place and temporal cues using cochlear implants" *J. Accoust. Soc. Am*, vol. 131, no. 2, pp. 1325-1336, 2012

[7] N. H. Lovell, S. Dokos, P. Preston, T. Lehmann, N. Dommel, A. Lin, Y. T Wong, N. L, Opie, L. E. Hallum, S. Chen, G. J. Suaning, "A retinal neuroprosthesis design based on simultaneous current injection", *Proceedings of the 3rd Annual International IEEE EMBS*, Kahuku, Hawaii, 12-15th May, 2005.

[8] R. Plonsey, "Volume conductor theory," in *The Biomedical Engineering Handbook*, J. D. Bronzino, Ed. Florida: CRC Press, 1995, pp. 119-125

[9] B. Roth. "The electrical properties of tissues" in *The Biomedical Engineering Handbook*, J. D. Bronzino, Ed. Florida: CRC Press, 1995, pp. 126-138